

Galacturonosyltransferase (GAUT)1 and GAUT7 are the core of a plant cell wall pectin biosynthetic homogalacturonan–galacturonosyltransferase complex

Melani A. Atmodjo^{a,b}, Yumiko Sakuragi^{c,d,1}, Xiang Zhu^{a,1}, Amy Joy Burrell^a, Sushree S. Mohanty^{a,e}, James A. Atwood III^{a,2}, Ron Orlando^a, Henrik Vibe Scheller^{c,f}, and Debra Mohnen^{a,b,e,3}

^aComplex Carbohydrate Research Center, ^bDepartment of Biochemistry and Molecular Biology, and ^eBioEnergy Science Center, University of Georgia, Athens, GA 30602; ^cDepartment of Plant Biology and Biotechnology and ^dVKR Research Centre Pro-Active Plants, University of Copenhagen, DK-1871 Frederiksberg C, Copenhagen, Denmark; and ^fJoint BioEnergy Institute, Lawrence Berkeley National Laboratory, Emeryville, CA 94608

Edited* by Deborah P. Delmer, The Rockefeller Foundation, New York, NY, and approved October 19, 2011 (received for review August 16, 2011)

Plant cell wall pectic polysaccharides are arguably the most complex carbohydrates in nature. Progress in understanding pectin synthesis has been slow because of its complex structure and difficulties in purifying and expressing the low-abundance, Golgi membrane-bound pectin biosynthetic enzymes. *Arabidopsis* galacturonosyltransferase 1 (GAUT1) is an α -1,4-galacturonosyltransferase that synthesizes homogalacturonan (HG), the most abundant pectic polysaccharide. We now show that GAUT1 functions in a protein complex with the homologous galacturonosyltransferase 7 (GAUT7). Surprisingly, although both GAUT1 and GAUT7 are type II membrane proteins with single N-terminal transmembrane-spanning domains, the N-terminal region of GAUT1, including the transmembrane domain, is cleaved in vivo. This raises the question of how the processed GAUT1 is retained in the Golgi, the site of HG biosynthesis. We show that the anchoring of GAUT1 in the Golgi requires association with GAUT7 to form the GAUT1–GAUT7 complex. Proteomics analyses also identified 12 additional proteins that immunoprecipitate with the GAUT1–GAUT7 complex. This study provides conclusive evidence that the GAUT1–GAUT7 complex is the catalytic core of an HG- α -1,4-galacturonosyltransferase complex and that cell wall matrix polysaccharide biosynthesis occurs via protein complexes. The processing of GAUT1 to remove its N-terminal transmembrane domain and its anchoring in the Golgi by association with GAUT7 provides an example of how specific catalytic domains of plant cell wall biosynthetic glycosyltransferases could be assembled into protein complexes to enable the synthesis of the complex and developmentally and environmentally plastic plant cell wall.

Pectin is the most structurally complex plant cell wall polysaccharide, requiring at least 67 transferases for synthesis (1, 2). It comprises ~35% of the primary wall in dicots and non-graminaceous monocots, and 2–10% in grasses (2). Pectin is a family of polysaccharides including homogalacturonan (HG), rhamnogalacturonan I (RG-I), rhamnogalacturonan II (RG-II), and xylogalacturonan, which are defined by the presence of α -D-galactopyranosyluronic acid (GalA) with sugar substituents at O-4 and O-1. Pectins have multiple functions in plant growth, development, and disease resistance including roles in cell–cell adhesion, wall porosity, cell elongation, and wall extensibility (3–6). They provide structural support in primary walls, influence secondary wall formation in fibers and woody tissues, and are a reservoir of oligosaccharide signaling molecules (1, 7–9). The gelling and stabilizing properties of pectin are exploited for food enhancement and industrial purposes, and pectin has multiple health benefits including lowering cholesterol and serum glucose levels, inhibiting cancer growth and metastasis, and prebiotic function in the gut (10–13).

HG is the most abundant pectic domain, comprising ~55–70% of pectin. HG is a linear homopolymer of α -1,4-linked GalA that is partially methyl-esterified at C-6 and O-acetylated at O-2/O-3, modifications that affect pectin structure and function (3). α -1,4-Galacturonosyltransferase (GalAT; EC 2.4.1.43) catalyzes transfer of GalA from uridine-diphosphate-GalA (UDP-GalA) onto

HG acceptors (14). HG–galacturonosyltransferase 1 (GAUT1) was identified by tandem mass spectrometry (MS) of *Arabidopsis* solubilized membrane preparations enriched for GalAT activity; transient expression in HEK293 cells; and immunoadsorption of GalAT activity from SP Sepharose-purified *Arabidopsis* solubilized membrane fractions (SP fraction) using anti-GAUT1 antibodies (15). GAUT1 encodes a protein of 673 amino acids (aa), predicted mass of 77.4 kDa, pI of 9.95, and type II transmembrane topology, consistent with Golgi localization of GAUT1 and HG–GalAT activity (16, 17). GAUT1 belongs to glycosyltransferase (GT) family 8 and the *Arabidopsis* GAUT1-related superfamily of 15 GAUT and 10 GAUT-like genes (15, 18–20).

GAUT7, another GAUT family member, was the only predicted GT that copurified with GAUT1 in GalAT-enriched detergent-solubilized *Arabidopsis* membrane proteins from suspension culture cells (15). Despite 36% aa sequence identity to GAUT1, GAUT7 had no HG–GalAT activity when transiently expressed in HEK293 cells (15), raising the question of whether GAUT7 functions in a biosynthetic complex with GAUT1. Here we show that *Arabidopsis* GAUT1 and GAUT7 form a GAUT1–GAUT7 HG–GalAT complex and that GAUT7 anchors a proteolytically processed form of GAUT1 in the Golgi.

Results and Discussion

GAUT7 Associates with GAUT1 in an HG–GalAT Complex. Polyclonal antibodies against amino acid positions 82–103 of *Arabidopsis* GAUT7 predicted stem region recognized a broad doublet band of ~75 kDa, confirmed to be GAUT7 by MS sequencing (Fig. 1A and Fig. S1 B and D). Immunoadsorption of GAUT7 from the *Arabidopsis* SP fraction using anti-GAUT7 antibodies caused an antibody-dependent depletion of GalAT activity from the supernatant and recovery of GalAT activity in the anti-GAUT7-immunoadsorbed pellet (Fig. S1A). The results suggested that GAUT7 was either a GalAT or part of a GalAT complex. Protein complexes involved in N-linked glycoprotein, glycolipid, and proteoglycan syntheses have been reported (21) and demonstrated or suggested in plant starch, cellulose, and hemicellulose syntheses (22–24). However, molecular analysis of a plant wall matrix polysaccharide biosynthetic complex has not been reported. To test whether GAUT7 exists in a GalAT complex with GAUT1, independent anti-GAUT1- and anti-GAUT7-immunoadsorbed proteins were separated by reducing SDS/PAGE and

Author contributions: M.A.A., Y.S., X.Z., J.A.A., R.O., H.V.S., and D.M. designed research; M.A.A., Y.S., X.Z., A.J.B., and S.S.M. performed research; M.A.A., Y.S., X.Z., A.J.B., J.A.A., and D.M. analyzed data; and M.A.A., Y.S., X.Z., J.A.A., H.V.S., and D.M. wrote the paper. The authors declare no conflict of interest.

*This Direct Submission article had a prearranged editor.

¹Y.S. and X.Z. contributed equally to this work.

²Present address: NuSep, Inc., Bogart, GA 30622.

³To whom correspondence should be addressed. E-mail: dmohnen@ccrc.uga.edu.

This article contains supporting information online at www.pnas.org/lookup/suppl/doi:10.1073/pnas.1112816108/-DCSupplemental.

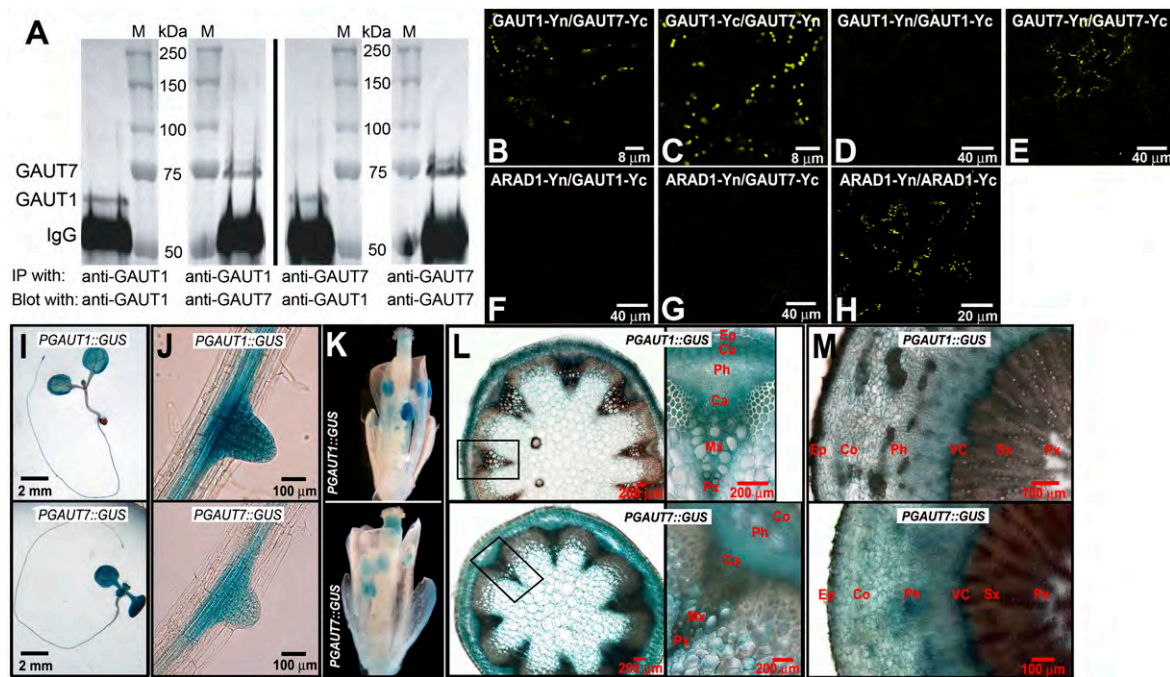


Fig. 1. GAUT1 and GAUT7 interact in a protein complex. (A) Coimmunoprecipitation of GAUT1 and GAUT7. Anti-GAUT1 and anti-GAUT7 antibody-immunoadsorbed proteins from the *Arabidopsis* SP fraction separated by SDS/PAGE and immunoblotted with anti-GAUT1 or anti-GAUT7 sera. The experiment was done thrice with similar results. IgG, IgG heavy chain detected by secondary antibody; IP, immunoprecipitation; M, molecular mass protein marker. (B–H) BiFC analysis of GAUT1 and GAUT7. Constructs were transiently coexpressed in *N. benthamiana* leaves, with BiFC of ARAD1 as control (28). YFP signals are in yellow. Individual expression of each construct gave no YFP signal. Results were verified by three independent experiments (except ARAD1 negative control, which was done twice). (I–M) *Arabidopsis* GAUT1 and GAUT7 promoter–GUS construct expression in whole (I) and developing lateral roots (J) of 7-d-old seedlings, and in flowers (K), stems (L), and tap roots (M) of mature 6- to 8-wk-old plants. Similar results were observed in multiple T2 plants from at least five independent T1 lines. Ca, cambium; Co, cortex; Ep, epidermis; Mx, metaxylem; Ph, phloem; Px, protoxylem (L) or primary xylem (M); Sx, secondary xylem; VC, vascular cambium.

Embargoed

analyzed by immunoblotting using anti-GAUT1 and anti-GAUT7 sera. *Arabidopsis* GAUT1 and GAUT7 coimmunoprecipitated from the SP fraction (Fig. 1A and Fig. S1), demonstrating biochemically that GAUT1 and GAUT7 exist in a protein complex.

Because protein colocalization within the same cellular subcompartment is a prerequisite for complex formation, we used bimolecular fluorescence complementation (BiFC) (25) to test for GAUT1 and GAUT7 colocalization in the Golgi. Transient expression in tobacco (*Nicotiana benthamiana*) leaves of GAUT7 fused to full-length YFP yielded punctate signals overlapping with those of the Golgi marker STmd-GFP (26) (see below) and indicating Golgi localization of GAUT7. GAUT1 fused to full-length GFP was also tested, but did not give any signals (see below). Fluorescence complementation with characteristic Golgi signal morphology was observed upon transient coexpression of GAUT1 and GAUT7, each fused to complementary split halves of YFP (Fig. 1B and C). Neither GAUT1 nor GAUT7 constructs complemented fluorescence with ARAD1-Yn [ARABINAN DEFICIENT 1 (27)], whereas the positive control ARAD1-Yn/ARAD1-Yc did fluoresce (Fig. 1F–H). Coexpression of GAUT1-Yn/GAUT1-Yc yielded no signal (Fig. 1D), whereas that of GAUT7-Yn/GAUT7-Yc gave variable fluorescence (Fig. 1E). The specific fluorescence complementation between GAUT1 and GAUT7 confirms that these proteins colocalize within a specific Golgi subcompartment and supports their association in a protein complex.

To determine whether *GAUT1* and *GAUT7* are coexpressed in *Arabidopsis*, we analyzed *Arabidopsis* gene expression databases and *GAUT1* and *GAUT7* promoter–GUS construct expression in transgenic *Arabidopsis*. Microarray data (<https://www.genevestigator.com>) show similar expression patterns of *GAUT1* and *GAUT7* in all plant tissues, with Pearson correlation coefficients (*r* values) of 0.600 and 0.684 from the Gene Co-Expression Analysis Toolbox (<http://genecat.mpg.de>) and *Arabidopsis* Co-Expression Analysis

Tool (<http://www.cressexpress.org>), respectively (see below). Promoter–GUS fusions (Fig. 1I–M) indicate high expression of both genes in meristematic regions, vascular tissues, and reproductive organs, and support a role for both proteins in primary and secondary wall syntheses. Extensive coexpression was observed in seedling cotyledon tips and vasculature, leaf primordia and outer edges of young leaves, and 6- to 8-wk-old plant cambium, phloem, epidermis, cortex, stem metaxylem and protoxylem, anthers, pollen, floral distal stigma, and root vascular cambium and phloem. The coexpression of *GAUT1* and *GAUT7* is consistent with their function in a protein complex.

The immunoprecipitated GAUT1–GAUT7 complex (Fig. 1A and Fig. S1) transfers GalA from UDP-GalA onto HG oligosaccharide (oligogalacturonide; OGA) acceptors, similar to the reported GalAT activity in solubilized membrane preparations (14). To test whether the GAUT1–GAUT7 complex transfers GalA onto RG-I and/or RG-II acceptors, substrate specificity was examined by comparing OGAs of degrees of polymerization (DP) 7–23; RG-I backbone oligomers of DP 6–26 with either a rhamnosyl residue (RG-I-R) or a GalA residue (RG-I-G) at the non-reducing end; and RG-II monomer. Fig. 2A shows that the immunoprecipitated GAUT1–GAUT7 complex, as well as GalAT activity in the *Arabidopsis* SP fraction, is highly selective for OGAs, verifying the GAUT1–GAUT7 complex as HG–GalAT.

GAUT1–GAUT7 Complex Is Held Together by Both Covalent and Non-covalent Interactions. Some GT complexes are known to contain disulfide bonds (29). We tested whether GAUT1 and GAUT7 associated via disulfide bonds by separating proteins from the *Arabidopsis* SP fraction on reducing versus nonreducing SDS/PAGE followed by Western blotting (Fig. 2B). GAUT1 and GAUT7 migrated as monomers when separated by reducing SDS/PAGE (~60 kDa for GAUT1; ~75 kDa for GAUT7).

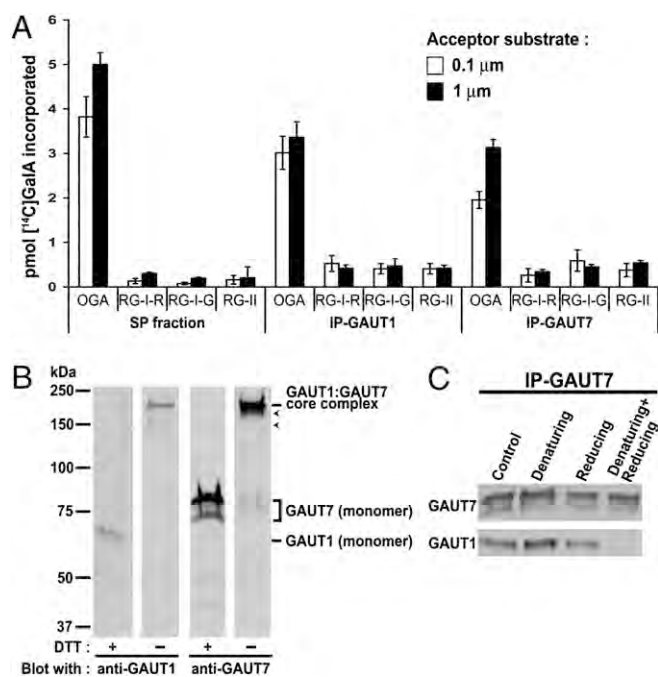


Fig. 2. The GAUT1–GAUT7 GalAT complex is selective for HG substrate and held together by covalent and noncovalent interactions. (A) GalAT activities of the *Arabidopsis* SP fraction and of anti-GAUT1- and anti-GAUT7-immunoprecipitated GAUT1–GAUT7 complex were tested at 0.1 and 1 μ M pectic acceptors: OGA DP 7–23; RG-I oligomers DP 6–26 with either rhamnose (RG-I-R) or GalA (RG-I-G) at the nonreducing ends; and RG-II monomer. Data are mean \pm SD ($n = 3$). (B) GAUT1 and GAUT7 resolve at higher masses in non-reducing SDS/PAGE. The *Arabidopsis* SP fraction separated by SDS/PAGE in the presence or absence of 25 mM DTT and analyzed by immunoblotting with anti-GAUT1 or anti-GAUT7 sera. Protein bands common to GAUT1 and GAUT7 are estimated at \sim 185 kDa (noted as GAUT1–GAUT7 core complex). Arrowheads indicate additional GAUT1 or GAUT7 HMW protein bands. (C) Coimmunoprecipitation of GAUT1 and GAUT7 is abolished only in the presence of both denaturing and reducing agents. The *Arabidopsis* SP fraction was preincubated for 30 min under denaturing [0.05% (vol/vol) Nonidet P-40, 0.0125% (wt/vol) deoxycholate, 0.5% (wt/vol) SDS], reducing (50 mM DTT), or both denaturing and reducing conditions before immunoprecipitation using anti-GAUT7 antibody and subsequent Western analysis.

However, both proteins resolved at a similar (\sim 185 kDa) high molecular weight (HMW) upon nonreducing SDS/PAGE, suggesting that GAUT1 and GAUT7 are held together by an intermolecular disulfide bond(s) in a common heterocomplex. To confirm that disulfide bonding indeed held GAUT1 and GAUT7 in a heterocomplex, we performed immunoprecipitation of the GAUT1–GAUT7 complex from the *Arabidopsis* SP fraction pretreated with denaturing agents, a reducing agent, or both denaturing and reducing agents (Fig. 2C). The GAUT1–GAUT7 complex remained intact under denaturing or reducing conditions alone, but dissociated when both denaturing and reducing agents were present. This result establishes covalent intermolecular disulfide bonding between GAUT1 and GAUT7, whereas noncovalent interactions may reinforce the integrity of the disulfide-bonded complex.

Proteomics Analyses Establish GAUT1 and GAUT7 as Components of the GAUT1–GAUT7 Core Complex and Identify Putative Interacting Proteins. We used repetitive high-stringency proteomics to identify components of the GAUT1–GAUT7 complex held together by covalent and noncovalent interactions (outlined in Fig. S2; Table 1). The complex was immunoprecipitated independently using antigen-purified anti-GAUT1- and anti-GAUT7-specific IgGs, each covalently attached to magnetic beads. After stringent

washing, the immunoprecipitants were eluted from the beads and resolved by SDS/PAGE (Materials and Methods).

To examine the minimal, disulfide-bonded GAUT1–GAUT7 complex, stable upon nonreducing SDS/PAGE, the \sim 185-kDa protein band of the GAUT1–GAUT7 core complex was excised from the gel (Fig. S3A), in-gel trypsin-digested, and subjected to liquid chromatography-tandem mass spectrometry (LC-MS/MS). GAUT1 and GAUT7 were the only two proteins identified by LC-MS/MS in each independent anti-GAUT1- and anti-GAUT7-specific IgG immunoprecipitant (IP-GAUT1 and IP-GAUT7, respectively; Table S1 and Dataset S1). Neither GAUT1 nor GAUT7 was detected in the preimmune IgG immunoprecipitation control (IP-control). The results establish that the non-reducing SDS/PAGE-stable complex consists only of GAUT1 and GAUT7. Based on the size of the complex observed in non-reducing SDS/PAGE and the normalized spectral abundance factor (NSAF) values of GAUT1 and GAUT7 from the LC-MS/MS data (Table S1), the GAUT1–GAUT7 core complex is likely to be a trimeric complex consisting of two GAUT1 subunits (each 58.6-kDa; see next section) and one GAUT7 subunit (69.7-kDa).

We reasoned that the minimal, disulfide-bonded GAUT1–GAUT7 complex may be a core complex associating noncovalently with additional proteins to form a larger pectin synthesis complex, for example with methyltransferases to synthesize methyl-esterified HG. Indeed, the size of detergent-solubilized polygalacturonic acid synthase (synonymous with HG–GalAT) from azuki bean was estimated as \sim 590 kDa (30). To test for possible GAUT1–GAUT7 core complex-associating proteins, eluted immunoprecipitants were resolved by reducing SDS/PAGE and analyzed by LC-MS/MS (Table S2 and Dataset S1). Because preliminary data showed immunoprecipitated proteins from \sim 50 to 125 kDa, we focused on these for the proteomics analyses (Fig. S3B). Ten proteins, including GAUT1 and GAUT7, were consistently identified in each IP-GAUT1 and IP-GAUT7 immunoprecipitant, but not in the IP-control (using preimmune IgG), as determined using two high-stringency proteomics data-filtering methods (i.e., false-discovery rate and probability analyses; Table S2 and SI Results and Discussion). Four other proteins were more than fourfold more abundant in IP-GAUT1 and IP-GAUT7 than in the IP-control (Table S2 and SI Results and Discussion). The 14 proteins, including GAUT1 and GAUT7, represent the GAUT1–GAUT7 core complex and its putative associating proteins (Table 1). Although it remains possible that all or some of the 14 proteins form a large holocomplex, the relatively low NSAF values of the 12 additional proteins compared with GAUT1 and GAUT7 suggest that they may transiently interact with the GAUT1–GAUT7 core complex.

Several GAUT1–GAUT7 core complex putative associating proteins are noteworthy. The two dehydration-responsive proteins (AT4G18030, AT4G00740) contain a putative methyltransferase domain (DUF248; InterPro IPR004159) and have homology (30–37% aa sequence identity, 47–55% similarity) to QUA2, a putative homogalacturonan-methyltransferase (HG-MT) (31). Recently, AT4G00740 has also been proposed as a putative HG-MT, designated QUA3 (32). AT4G18030 and AT4G00740 have been localized to the Golgi (17), as has HG-MT activity (33), and are coexpressed with GAUT1 and GAUT7 (Table S3). These results support the proposition that methylation of HG occurs as it is synthesized, or immediately thereafter (1, 2). The presence of KORRIGAN1 (KOR1/AT5G49720), a membrane-bound endo-1,4- β -glucanase implicated in cellulose biosynthesis (22), as a GAUT1–GAUT7 complex putative associating protein warrants further investigation. *KOR1* mutants are dwarf, defective in cell elongation, and have reduced wall crystalline cellulose that is compensated by increased pectin (34). *KOR1* localizes to a heterogeneous population of intracellular compartments including the Golgi (22). Perhaps most intriguingly, two homologs of mammalian ribophorins I and II (AT1G76400 and AT4G21150, respectively) are among the putative GAUT1–GAUT7 complex-interacting proteins. These ribophorins are subunits of oligosaccharyltransferase, an enzyme complex that transfers oligosaccharides *en bloc* from

Table 1. The GAUT1–GAUT7 GalAT core complex and putative associating proteins as revealed by proteomics analyses of the immunoprecipitated complex

Protein ID	Gene ID	Sequence name	Protein length (aa)	Protein mass (kDa)	IP-GAUT1			IP-GAUT7						
					Total protein probability	Total score	Total spectra	Corrected NSAF value [†]	Total protein probability	Total score	Total spectra	Corrected NSAF value [†]		
GAUT1–GAUT7 nonreducing SDS/PAGE-stable core complex														
NP_191672.1	At3g61130	GAUT1/LGT1 (Galacturonosyltransferase 1)	673	77.31	1	530.98	19	0.555	0.625	1	256.18	8	0.434	0.583
NP_565893.1	At2g38650	GAUT7/LGT7 (Galacturonosyltransferase 7)	619	69.69	1	362.67	14	0.445	0.375	1	196.85	7	0.417	0.417
GAUT1–GAUT7 core complex and putative associating proteins														
NP_191672.1	At3g61130	GAUT1/LGT1 (Galacturonosyltransferase 1)	673	77.31	1	1573.58	122	0.073	0.095	1	2013.38	228	0.047	0.061
NP_565893.1	At2g38650	GAUT7/LGT7 (Galacturonosyltransferase 7)	619	69.69	1	1372.61	167	0.111	0.107	1	1668.63	327	0.072	0.071
NP_176170.1	At1g59610	ADL3 (ARABIDOPSIS DYNAMIN-LIKE 3)	920	100.15	1	973.23	48	0.020	0.021	1	1083.70	64	0.009	0.009
NP_177766.1	At1g76400	Ribophorin I family protein	614	68.58	1	780.90	41	0.026	0.026	1	980.38	143	0.032	0.031
NP_172500.1	At1g10290	ADL6 (DYNAMIN-LIKE PROTEIN 6)	914	99.09	1	736.39	36	0.015	0.016	1	1000.20	68	0.010	0.010
NP_193537.2	At4g18030	Dehydration-responsive family protein	621	70.27	1	721.96	25	0.016	0.016	1	612.05	42	0.009	0.009
NP_193847.2	At4g21150	Ribophorin II (RPN2) family protein	691	74.60	1	641.43	19	0.011	0.011	1	1098.01	65	0.013	0.013
NP_190258.1	At3g46740	TOC75-III (translocon outer-membrane complex 75-III)	818	89.12	1	608.83	28	0.014	0.013	1	747.03	49	0.008	0.008
NP_186956.2	At3g03060	ATPase	628	69.51	1	541.41	30	0.019	0.019	1	513.82	58	0.013	0.012
NP_179673.1	At2g20800	NDB4 [NAD(P)H DEHYDROGENASE B4]	582	65.31	1	487.12	17	0.011	0.012	1	1093.47	117	0.027	0.027
NP_565435.1	At2g18330	AAA-type ATPase family protein	636	71.13	1	423.99	36	0.023	0.022	1	765.71	105	0.023	0.022
NP_188616.1	At3g19820	DWF1 (DIMINUTO 1)	561	65.33	1	409.62	15	0.010	0.011	1	901.14	112	0.027	0.027
NP_567184.1	At4g00740	Dehydration-responsive protein-related	600	67.49	1	385.40	13	0.009	0.009	1	549.74	36	0.008	0.008
NP_199783.1	At5g49720	KOR1 (KORRIGAN)	621	69.13	1	229.31	9	0.006	0.006	1	243.22	15	0.003	0.003

Proteomics analyses were conducted on multiple independent sets of immunoprecipitations performed using anti-GAUT1–IGG (IP-GAUT1), anti-GAUT7–IGG (IP-GAUT7), and preimmune IgG (IP-control) (see details in *SI Text*). GAUT1 and GAUT7 are the only identified components of the nonreducing SDS/PAGE-stable core complex, whereas 14 proteins, including GAUT1 and GAUT7, constitute the GAUT1–GAUT7 GalAT complex and its putative associating proteins. Data shown are proteins reproducibly identified in both IP-GAUT1 and IP-GAUT7, and not in IP-control, based on probability analysis. The putative associating proteins also include those more than fourfold more abundant in IP-GAUT1 and IP-GAUT7 compared with IP-control. Proteins are listed based on total protein scores in the IP-GAUT1 datasets. Total probability: the estimate of the likelihood that the protein assignment is correct based on the peptide probabilities for the identified peptides mapping to the protein. Total score: the sum of the peptide scores (Mascot ion scores) for all peptides matching to a protein. Total spectra: the sum of all spectra generating peptide identifications to a given protein, that is, the number of redundant protein spectra.

*NSAF values are protein normalized spectral counts, calculated as the number of spectral counts for protein X (SpC) divided by the number of amino acids in protein X (L) divided by the sum of SpC/L for all proteins in the experimental dataset.

[†]Corrected NSAF values were calculated based on the size of the cleaved GAUT1, that is, 506-aa long.

dolichol pyrophosphates onto proteins as they translocate into the endoplasmic reticulum (ER) lumen (35). The identification of the ribophorins raises the possibility that biosynthesis of HG, or of pectin in general, may occur by *en bloc* transfer of oligosaccharide domains to a growing polysaccharide.

GAUT1 Is Posttranslationally Cleaved. *Arabidopsis* GAUT1 is predicted to be a 77.4-kDa protein, yet always resolved at ~60 kDa (15) (Figs. 1A and 2B and Fig. S1). We proposed that the discrepancy between the predicted and observed sizes of GAUT1 was the result of posttranslational proteolytic processing *in planta*. This was tested using three independent anti-GAUT1 antibodies, reactive against GAUT1 amino acid positions 132–154, 341–365, and 448–472 (ref. 15 and this paper). Whereas all three antibodies detected recombinant GAUT1 expressed in HEK293 cells (15), only the antibodies generated against amino acids 341–365 and 448–472 recognized GAUT1 in immunoblots of the *Arabidopsis* SP fraction (Fig. S4), suggesting that *Arabidopsis* GAUT1 is proteolytically cleaved *in vivo* in the N-terminal region.

N-terminal sequencing of GAUT1 excised from a reducing SDS/PAGE-blotted membrane yielded the peptide sequence

RANELVQ, indicating a cleavage between Met₁₆₇ and Arg₁₆₈ that yields a processed *Arabidopsis* GAUT1 of 58.6 kDa and pI of 9.3, consistent with the observed characteristics of GAUT1 in the SP fraction. The cleavage site was also supported by LC-MS/MS analyses of immunoprecipitated GAUT1–GAUT7 complex, which gave no GAUT1 peptide sequence N-terminal to Ala₁₆₉ (Fig. S3 C and D). The GAUT1 aa sequence surrounding this proposed cleavage site is consistent with the consensus motif ([R/K]–[X]_n–[R/K], *n* = 0, 2, 4, or 6) recognized by subtilisin-like proprotein convertases in the secretory pathway (36). Proteolytic cleavage at stem regions by secretory pathway proteases has been documented with many other GTs (29, 37). Whereas the resulting soluble, truncated GTs are typically secreted out of the cell, the *N*-glycosylation enzyme GlcNAcT-I was reported cleaved but retained in the Golgi via inclusion in HMW oligomers mediated by its luminal domain (38). GAUT1 cleavage *in planta* could activate the enzyme, as described for *Arabidopsis* and tobacco type I pectin methyltransferases (39), or could facilitate specific GAUT1 and GAUT7 association to form the GAUT1–GAUT7 core complex and/or a larger, fully functional pectin biosynthetic

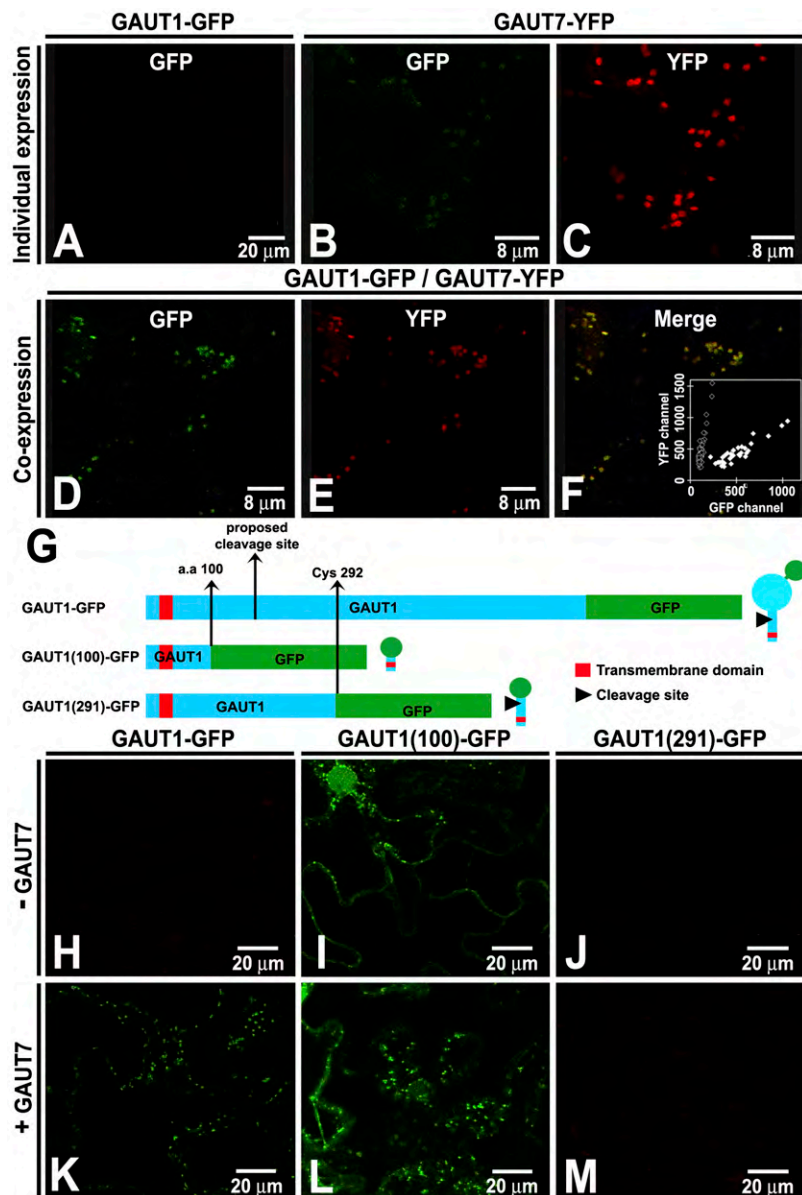


Fig. 3. Golgi retention of cleaved GAUT1 relies on the presence of GAUT7. (A–F) Transient coexpression of GAUT1-GFP and GAUT7-YFP in *N. benthamiana* leaves. (F, Inset) Mean pixel intensity is plotted from each Golgi in the GFP versus YFP channels (detected by sequential scanning), showing Golgi signals in GAUT1-GFP individual expression experiments (◊) and GAUT1-GFP/GAUT7-YFP coexpression experiments (◆). The Inset reveals that GFP signals detected upon GAUT1-GFP/GAUT7-YFP coexpression (D) are caused by the Golgi accumulation of GAUT1-GFP in the presence of GAUT7-YFP, and not to background signal from GAUT7-YFP (B). Results were verified in at least three independent experiments. (G–M) Transient expression of C-terminally truncated GAUT1-GFP fusion constructs (G) in the absence (H–J) or presence (K–M) of GAUT7. GAUT1-GFP, full-length GAUT1 fused to GFP; GAUT1(100)-GFP, first 100 aa of GAUT1 fused to GFP; GAUT1(291)-GFP, first 291 aa of GAUT1 fused to GFP.

complex. Further studies are needed to establish the function(s) of GAUT1 processing.

GAUT1 Is Dependent on GAUT7 for Retention in the Golgi. A cleavage between Met₁₆₇ and Arg₁₆₈ would render GAUT1 devoid of its transmembrane domain (TMD) and thus secreted out of the cell unless a tethering mechanism retained it in the Golgi. We hypothesized that interaction with GAUT7 retained GAUT1 in the Golgi. To test this, GAUT1-GFP and GAUT7-YFP constructs were individually and coexpressed in tobacco leaves. When individually expressed, GAUT1-GFP did not yield a Golgi signal (Fig. 3A), whereas GAUT7-YFP did (Fig. 3C). However, when coexpressed, accumulation of GAUT1-GFP in the Golgi overlapped with GAUT7-YFP signal (Fig. 3D–F). GAUT1-GFP also accumulated in the Golgi when coexpressed with nontagged GAUT7 (Fig. 3H and K). The results demonstrate that retention of GAUT1 in the Golgi requires the presence of GAUT7, and suggest that GAUT7 acts as a membrane anchor for GAUT1.

To further explore the GAUT1 tethering mechanism, three GAUT1-GFP fusion constructs (Fig. 3G) were transiently expressed in tobacco with and without coexpressed nontagged GAUT7. The constructs were (i) GAUT1-GFP (GAUT1 full-length), (ii) GAUT1(100)-GFP containing only the first 100 aa of GAUT1 including the predicted TMD but not the proposed cleavage site, and (iii) GAUT1(291)-GFP containing the first 291 aa of GAUT1 including both the predicted TMD and cleavage site but not the first cysteine beyond the predicted TMD (Cys₂₉₂). Transient expression of GAUT1-GFP yielded GAUT7-dependent fluorescence accumulation in Golgi (Fig. 3H and K and Fig. S5B–E). In contrast, despite the absence or presence of GAUT7, GAUT1(100)-GFP yielded a broad labeling pattern, including ER and punctate Golgi-like structures (Fig. 3I and L), whereas GAUT1(291)-GFP accumulated no observable signal (Fig. 3J and M and Fig. S5B–E). GAUT1(100)-GFP seems sufficient to target the protein to the secretory pathway but does not provide Golgi-specific localization. GAUT1(291)-GFP, however, likely underwent proteolytic cleavage, releasing the C-terminally located GFP from the membrane and resulting in secretion into the apoplast, where GFP generates weak or no fluorescence because of the low-pH environment (40). The results indicate a cleavage site between amino acids 100 and 291, consistent with the proposed cleavage site between Met₁₆₇ and Arg₁₆₈, suggest the importance of disulfide bonding between GAUT1 and GAUT7 to retain GAUT1 in the Golgi, and indicate a region downstream of amino acid 291 in GAUT1 as required for specific protein–protein interactions between GAUT1 and GAUT7.

Model for the GAUT1–GAUT7 HG–GalAT Core Complex. Based on all of the data presented, we propose a heterotrimeric model for the GAUT1:–GAUT7 core complex (Fig. 4) of GAUT1 and GAUT7 held together by a covalent disulfide bond(s) and other noncovalent

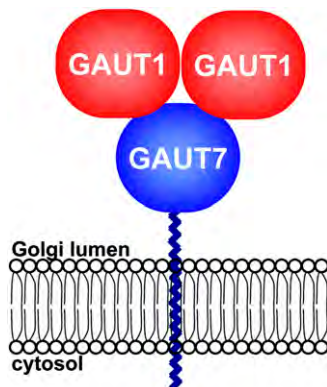


Fig. 4. A model of the *Arabidopsis* GAUT1–GAUT7 core complex.

interactions. GAUT1 and GAUT7 each contain eight cysteine residues (two and six in the TMD and luminal region, respectively). One or more of these is proposed to function in disulfide-bond formation. GAUT1 is the catalytic subunit (15) of the GAUT1–GAUT7 HG–GalAT complex. GAUT7 functions, at least in part, to anchor GAUT1 to the Golgi membrane. Interestingly, it was reported that GAUT7 carries an amino acid substitution in a proposed catalytic residue that would render it noncatalytic (20). This proposition needs experimental verification, but is consistent with a GAUT1-anchoring, noncatalytic role for GAUT7.

Heterocomplex formation of closely related GTs has been shown to have functional significance. For examples, proper folding of the mammalian *O*-glycosylation enzyme Clβ1,3-GalT in the ER requires complex formation with the homologous (22% identity) type II transmembrane protein Cosmc (41), whereas complex formation of human protein *O*-mannosyltransferases POMT1 and POMT2 (36% identity) is necessary for enzymatic activity of otherwise inactive subunits (42). Heterocomplex formation of the heparan sulfate biosynthetic enzymes EXT1 and EXT2 (35% identity) results in a Golgi-localized enzyme complex with significantly higher GlcNAcT/GlcAT activities than those of the individual components and with a polymerizing capability (43). It is plausible that the GAUT1–GAUT7 complex may have substantially higher catalytic and/or polymerizing activities compared with the individual subunits.

The work reported here indicates that pectin HG synthesis occurs via tethering of a GalAT catalytic subunit (GAUT1) to a Golgi membrane-bound protein anchor (GAUT7). How widespread this phenomenon is in the synthesis of cell wall polysaccharides remains to be determined. It is interesting to speculate, however, that Golgi-tethering proteins, such as GAUT7, may play a broader role in promoting the association of GTs and polysaccharide-modifying enzymes (such as methyltransferases) into complexes to achieve the synthesis of specific wall polysaccharide domains. In this regard, it is noteworthy that multiple GAUT7 homologs exist in the grass family (20), suggesting a unique role for GAUT7-like proteins in grasses. Further studies of the GAUT1–GAUT7 core complex and its associating proteins are likely to expand our view of how diverse GTs and polysaccharide-modifying enzymes interact to produce cell type- and developmental stage-specific wall polymers.

Materials and Methods

Immunoprecipitation. Anti-GAUT1 polyclonal antibodies were previously generated (15). Anti-GAUT7 antibodies were generated similarly using multiple antigenic peptides corresponding to GAUT7 amino acids 82–103 (DEVLQKINPVLPKKSDINVGSR). For coimmunoprecipitation of GAUT1 and GAUT7, 30 μL of anti-GAUT1 or anti-GAUT7 antibody-conjugated Dynabeads M-280 sheep anti-rabbit IgG (as described in ref. 15) were incubated with 500 μL SP fraction (SI Materials and Methods). Immunoabsorbed materials were washed twice in PBS, three times in buffer A [50 mM HEPES, pH 7.3, 0.25 mM MnCl₂, 2 mM EDTA, 25% (vol/vol) glycerol, 1% (vol/vol) Triton X-100], and once in PBS. PBS washes were done to remove nonspecific ionically interacting proteins, and to lower the Triton X-100 concentration below the critical micelle concentration to remove nonspecific proteins that may have associated via detergent micelles. Buffer A washes removed nonspecific, hydrophobically interacting proteins. Immunoprecipitants were analyzed by Western blotting with anti-GAUT1 and anti-GAUT7 sera (dilutions of 1:3,000 and 1:10,000, respectively). Immunoprecipitations for acceptor substrate specificity studies and of the SP fraction pretreated with denaturing and/or reducing conditions were as above, except that antibody beads and the SP fraction were incubated at 1:1 and 1:2 ratios (vol/vol), respectively.

GalAT Activity Assay for Substrate Specificity Studies. GalAT activity was measured as described (14) using size-specific HG, RG-I, and RG-II acceptors (see SI Materials and Methods for details).

BiFC and Coexpression of GAUT1 and GAUT7 Fused to Fluorescent Proteins. Bacterial strains, growth conditions, plasmid constructions, transfection of *N. benthamiana*, and settings for confocal microscopy are detailed in SI Materials and Methods.

Proteomics Analyses of the GAUT1–GAUT7 Complex. The experimental scheme is presented in Fig. S2. Independent experiments were done twice and three

times for studies of the nonreducing SDS/PAGE-stable core complex and the complex-associating proteins, respectively. In each independent proteomics experiment, three immunoprecipitations were carried out: IP-GAUT1, IP-GAUT7, and IP-control (using anti-GAUT1-specific IgG, anti-GAUT7-specific IgG, and total preimmune IgG, respectively). Antigen-purified specific IgGs (*SI Materials and Methods*) were covalently attached to Dynabeads M-270 Epoxy (Invitrogen) (450 μ g IgG per 22.5 mg beads). Immunoprecipitation was done by incubating IgG beads with 1.5 mL *Arabidopsis* SP fraction for 2 h at 4 °C with end-to-end rotation, followed by stringent washing (*Immunoprecipitation*). Immunoadsorbed proteins were eluted using 675 μ L of 100 mM glycine (pH 2.5) and neutralized by adding 75 μ L of 1 M Tris (pH 9.0). The procedure was repeated with the same IgG beads using fresh SP fraction (total of four and three times for the core complex and complex-associating proteins, respectively). Pooled eluted protein from each treatment was concentrated, and separated by 7.5% SDS/PAGE using nonreducing and reducing conditions to study the core complex and the complex-associating proteins, respectively. In-gel trypsin digestion and LC-MS/MS analyses are detailed in *SI Materials and Methods*. ProteoIQ version 1.5.02 software (<http://www.nusep.com>) was used to analyze the protein and

peptide identifications by separately using two statistical algorithms on board the software, namely the false-discovery rate and the probability methods (procedures and parameters are detailed in *SI Materials and Methods*).

Further information is provided in *SI Materials and Methods*.

ACKNOWLEDGMENTS. We thank Drs. Jae-Min Lim and Lance Wells for LC-MS/MS verification of GAUT1 and GAUT7; Drs. Alan Darvill, Michael Hahn, and Geert-Jan Boons for critical reading of the manuscript; Sarah Inwood, Carl Bergmann, and Henk Schols for gifts of enzymes; and Malcolm O'Neill for RG-II monomer. This work was supported by National Research Initiative, Cooperative State Research, Education, and Extension Service, US Department of Agriculture (USDA) Awards 2003-35318-15377 and 2006-35318-17301; USDA AFRI 2010-65115-20396; and in part by US Department of Energy (DOE) Contract DE-AC02-05CH11231, the Danish Agency for Science, Technology and Innovation, The Villum Kann Rasmussen Foundation, DOE Center Grant DE-FG02-09ER20097, and BioEnergy Science Center Grant DE-PS02-06ER64304. The BioEnergy Science Center is a US DOE BioEnergy Research Center supported by the Office of Biological and Environmental Research in the DOE Office of Science.

- Caffall KH, Mohnen D (2009) The structure, function, and biosynthesis of plant cell wall pectic polysaccharides. *Carbohydr Res* 344:1879–1900.
- Mohnen D (2008) Pectin structure and biosynthesis. *Curr Opin Plant Biol* 11:266–277.
- Willats WG, et al. (2001) Modulation of the degree and pattern of methyl-esterification of pectic homogalacturonan in plant cell walls. Implications for pectin methyl esterase action, matrix properties, and cell adhesion. *J Biol Chem* 276:19404–19413.
- Derbyshire P, McCann MC, Roberts K (2007) Restricted cell elongation in *Arabidopsis* hypocotyls is associated with a reduced average pectin esterification level. *BMC Plant Biol* 7:31.
- Ezaki N, Kido N, Takahashi K, Katou K (2005) The role of wall Ca^{2+} in the regulation of wall extensibility during the acid-induced extension of soybean hypocotyl cell walls. *Plant Cell Physiol* 46:1831–1838.
- O'Neill MA, Ishii T, Albersheim P, Darvill AG (2004) Rhamnogalacturonan II: Structure and function of a borate cross-linked cell wall pectic polysaccharide. *Annu Rev Plant Biol* 55:109–139.
- Lionetti V, et al. (2010) Engineering the cell wall by reducing de-methyl-esterified homogalacturonan improves saccharification of plant tissues for bioconversion. *Proc Natl Acad Sci USA* 107:616–621.
- Brutus A, Sicilia F, Macone A, Cervone F, De Lorenzo G (2010) A domain swap approach reveals a role of the plant wall-associated kinase 1 (WAK1) as a receptor of oligogalacturonides. *Proc Natl Acad Sci USA* 107:9452–9457.
- Singh B, et al. (2009) A specialized outer layer of the primary cell wall joins elongating cotton fibers into tissue-like bundles. *Plant Physiol* 150:684–699.
- Thakur BR, Singh RK, Handa AK (1997) Chemistry and uses of pectin—A review. *Crit Rev Food Sci Nutr* 37(1):47–73.
- Jackson CL, et al. (2007) Pectin induces apoptosis in human prostate cancer cells: Correlation of apoptotic function with pectin structure. *Glycobiology* 17:805–819.
- Behall K, Reiser S (1986) Effects of pectin on human metabolism. *Chemistry and Function of Pectins*, eds Fishman ML, Jen JJ (Am Chem Soc, Washington, DC), pp 248–465.
- Manderson K, et al. (2005) In vitro determination of prebiotic properties of oligosaccharides derived from an orange juice manufacturing by-product stream. *Appl Environ Microbiol* 71:8383–8389.
- Doong RL, Mohnen D (1998) Solubilization and characterization of a galacturonosyltransferase that synthesizes the pectic polysaccharide homogalacturonan. *Plant J* 13:363–374.
- Sterling JD, et al. (2006) Functional identification of an *Arabidopsis* pectin biosynthetic homogalacturonan galacturonosyltransferase. *Proc Natl Acad Sci USA* 103:5236–5241.
- Sterling JD, Quigley HF, Orellana A, Mohnen D (2001) The catalytic site of the pectin biosynthetic enzyme α -1,4-galacturonosyltransferase is located in the lumen of the Golgi. *Plant Physiol* 127:360–371.
- Dunkley TP, et al. (2006) Mapping the *Arabidopsis* organelle proteome. *Proc Natl Acad Sci USA* 103:6518–6523.
- Caffall KH, Pattathil S, Phillips SE, Hahn MG, Mohnen D (2009) *Arabidopsis thaliana* T-DNA mutants implicate GAUT genes in the biosynthesis of pectin and xylan in cell walls and seed testa. *Mol Plant* 2:1000–1014.
- Cantarel BL, et al. (2009) The Carbohydrate-Active EnZymes database (CAZy): An expert resource for glycogenomics. *Nucleic Acids Res* 37(Database issue):D233–D238.
- Yin Y, Chen H, Hahn MG, Mohnen D, Xu Y (2010) Evolution and function of the plant cell wall synthesis-related glycosyltransferase family 8. *Plant Physiol* 153:1729–1746.
- de Graffenried CL, Bertozzi CR (2004) The roles of enzyme localisation and complex formation in glycan assembly within the Golgi apparatus. *Curr Opin Cell Biol* 16:356–363.
- Taylor NG (2008) Cellulose biosynthesis and deposition in higher plants. *New Phytol* 178:239–252.
- Hannah LC, James M (2008) The complexities of starch biosynthesis in cereal endosperms. *Curr Opin Biotechnol* 19(2):160–165.
- Zeng W, et al. (2010) A glucurono(arabino)xylan synthase complex from wheat contains members of the GT43, GT47, and GT75 families and functions cooperatively. *Plant Physiol* 154(1):78–97.
- Hu CD, Chinenov Y, Kerppola TK (2002) Visualization of interactions among bZIP and Rel family proteins in living cells using bimolecular fluorescence complementation. *Mol Cell* 9:789–798.
- Boevink P, et al. (1998) Stacks on tracks: The plant Golgi apparatus traffics on an actin/ER network. *Plant J* 15:441–447.
- Harholt J, et al. (2006) ARABINAN DEFICIENT 1 is a putative arabinosyltransferase involved in biosynthesis of pectic arabinan in *Arabidopsis*. *Plant Physiol* 140(1):49–58.
- Sakuragi Y, Norholm MH, Scheller HV (2011) Visual mapping of cell wall biosynthesis. *Methods Mol Biol* 715:153–167.
- Young WW, Jr. (2004) Organization of Golgi glycosyltransferases in membranes: Complexity via complexes. *J Membr Biol* 198(1):1–13.
- Ohashi T, Ishimizu T, Akita K, Hase S (2007) In vitro stabilization and minimum active component of polygalacturonic acid synthase involved in pectin biosynthesis. *Biosci Biotechnol Biochem* 71:2291–2299.
- Mouille G, et al. (2007) Homogalacturonan synthesis in *Arabidopsis thaliana* requires a Golgi-localized protein with a putative methyltransferase domain. *Plant J* 50:605–614.
- Miao Y, Li HY, Shen J, Wang J, Jiang L (2011) QUASIMODO 3 (QUA3) is a putative homogalacturonan methyltransferase regulating cell wall biosynthesis in *Arabidopsis* suspension-cultured cells. *J Exp Bot* 62:5063–5078.
- Goubet F, Mohnen D (1999) Subcellular localization and topology of homogalacturonan methyltransferase in suspension-cultured *Nicotiana tabacum* cells. *Planta* 209(1):112–117.
- Mølhøj M, Pagant S, Höfte H (2002) Towards understanding the role of membrane-bound endo- β -1,4-glucanases in cellulose biosynthesis. *Plant Cell Physiol* 43:1399–1406.
- Kelleher DJ, Gilmore R (2006) An evolving view of the eukaryotic oligosaccharyltransferase. *Glycobiology* 16(4):47R–62R.
- Rholam M, Fahy C (2009) Processing of peptide and hormone precursors at the dibasic cleavage sites. *Cell Mol Life Sci* 66:2075–2091.
- El-Battari A, et al. (2003) Different glycosyltransferases are differentially processed for secretion, dimerization, and autoglycosylation. *Glycobiology* 13:941–953.
- Opat AS, Houghton F, Gleeson PA (2000) Medial Golgi but not late Golgi glycosyltransferases exist as high molecular weight complexes. Role of luminal domain in complex formation and localization. *J Biol Chem* 275:11836–11845.
- Wolf S, Rausch T, Greiner S (2009) The N-terminal pro region mediates retention of unprocessed type-I PME in the Golgi apparatus. *Plant J* 58:361–375.
- Zheng H, Kunst L, Hawes C, Moore I (2004) A GFP-based assay reveals a role for RHD3 in transport between the endoplasmic reticulum and Golgi apparatus. *Plant J* 37:398–414.
- Ju T, Cummings RD (2002) A unique molecular chaperone Cosmc required for activity of the mammalian core 1 β 3-galactosyltransferase. *Proc Natl Acad Sci USA* 99:16613–16618.
- Akasaka-Manyu K, Manyu H, Nakajima A, Kawakita M, Endo T (2006) Physical and functional association of human protein O-mannosyltransferases 1 and 2. *J Biol Chem* 281:19339–19345.
- Nadanaka S, Kitagawa H (2008) Heparan sulphate biosynthesis and disease. *J Biochem* 144(1):7–14.